

# Solid State NMR Investigations on Nanosized Carrier Systems

Christian Mayer<sup>1</sup> and Gerold Lukowski<sup>2,3</sup>

Received September 10, 1999; accepted January 7, 2000

**KEY WORDS:** Solid Lipid Nanoparticles; nuclear magnetic resonance (NMR); magic angle spinning (MAS); lineshape analysis; particle dynamics; rotational diffusion.

## INTRODUCTION

Nanosized drug delivery systems have been introduced in order to improve therapeutic efficacy by enabling controlled drug release, drug targeting or prolongation of circulation time. The development of nanoparticulate carriers presents a variety of challenges with regard to their comprehensive and time resolved analysis. A promising option is represented by nuclear magnetic resonance spectroscopy (NMR). The high resolution variety of this method is well known for its utility in the elucidation of complex chemical structures. On the other hand, wide-line NMR spectroscopy is particularly sensitive to the characteristics of molecular motion. Recently, an approach has been proposed (1) which combines a residual spectral resolution, in most cases sufficient to allow clear assignments of <sup>13</sup>C NMR signals, with the possibility to perform detailed line shape analyses yielding motional parameters. It is based on off-magic angle spinning, a variety of the more common method of magic angle spinning (MAS) NMR spectroscopy, which has been used for various purposes in previous studies (2–5). A well defined deviation from the magic angle (54.7°) yields a residual line broadening. The line broadening reduces spectral resolution to a certain extent but still allows spectral assignments of chemical components, while at the same time line shapes of the corresponding signals reflect dynamic parameters and may be analyzed for the mobility of individual components (1). In contrast to NMR methods which simply differentiate between mobile and immobile contributions, this method gives detailed information about the mobility of solid and dissolved constituents, overall particle sizes, and release processes. An important requirement is the stability of the sample with respect to the inertial field induced by the sample rotation. As an example for nanosized drug delivery systems, an aqueous suspension of solid lipid nanoparticles (SLN), which combine the advantage of low cytotoxicity (6) with the potential for large scale production was investigated.

## MATERIALS AND METHODS

### Preparation of Nanoparticles

The SLN were produced as described previously (7). The lipid cetylpalmitate used was purchased from Merck (Darmstadt, Germany) and the o/w-emulsifier Plantacare 2000 was provided by Henkel (Düsseldorf, Germany). The melted lipid was added to a mixture of twice distilled water and the surfactant Plantacare 2000. The mixture was stirred for 1 min with an Ultra-Turrax K18 (Jahnke and Kunkel GmbH, Staufen, Germany) at 9500 rpm. The preformulation was prepared by high pressure homogenization using a Micron LAB 40 homogenizer (APV Homogeniser GmbH, Lübeck, Germany).

### NMR Experiments and Analysis of Spectra

The aqueous suspension of solid lipid nanoparticles could be used without further preparation. It was filled into a 10 mm sample rotor which, had to be sealed tightly to avoid leakage of the liquid contents. The rotor was transferred into a commercial double-resonance MAS probe of an ASX 400 spectrometer (Bruker, Karlsruhe) and spun at an angle of 52.5° (2.2° deviation from the magic angle) and at a frequency of 1660 Hz. The applied pulse sequence consisted of a simple  $\pi/2$ -pulse (100.6 MHz for <sup>13</sup>C) of 7  $\mu$ s duration followed by an acquisition period on the <sup>13</sup>C-channel under <sup>1</sup>H decoupling for the full length of the free induction decay (FID). A total number of 20,000 scans was acquired at a recycle delay of 4 s and a sweep width of 30 kHz. The FID was Fourier transformed with exponential line broadening of 10 Hz.

The resulting spectral lineshapes were analyzed using a Fortran program for numeric simulation of sample spinning NMR spectra which has been described in detail elsewhere (1). The only adjustable parameter was the tumbling rate of the particles, all other parameters (spinning rate, spinning angle, tensor elements) were known. The correlation time  $\tau_r$  for the tumbling of the particles was varied until the best fit of experimental data was achieved.

### Photon Correlation Spectroscopy (PCS)

Particle size distributions were obtained by dynamic light scattering measurements at a fixed angle of 90° by using a Malvern Zetasizer 3000 HS (Malvern Instruments Ltd., Malvern, UK). The samples were prepared with dust-free water. An experimental autocorrelation function (EAF) was obtained as a result of the photon scattering spectroscopy. The experimental EAF was analysed using the Fortran program CONTIN (8). This program allowed to calculate multimodal size distributions of the nanoparticles. A number distribution was used for the interpretation of the data.

## RESULTS

The spectral lineshape obtained on solid lipid nanoparticles in aqueous suspension under off-magic angle sample spinning conditions is shown in Fig. 1. The baseline is distorted due to the background signal of the probe and the relative intensities of the peaks are shifted due to incomplete spin-lattice relaxation. Spinning sidebands, a typical phenomenon for sample spinning

<sup>1</sup> Institute for Physical and Theoretical Chemistry, University of Duisburg, 47048 Duisburg, Germany.

<sup>2</sup> Institute for Pharmacy, E.M. Arndt University, Jahnstr. 17, 17487 Greifswald, Germany.

<sup>3</sup> To whom correspondence should be addressed. (e-mail: lukowski@mail.uni-greifswald.de)

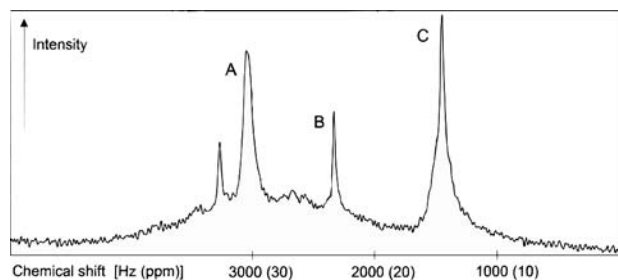


**Fig. 1.**  $^{13}\text{C}$  spectral lineshape obtained on solid lipid nanoparticles in aqueous suspension under off-magic angle sample spinning conditions and proton decoupling. The rotation axis is tilted at an angle of  $52.5^\circ$  which corresponds to a deviation of  $2.2^\circ$  from the magic angle. The baseline is distorted due to the background signal of the probe and the relative intensities of the peaks are shifted due to incomplete spin-lattice relaxation. Signal A corresponds to the majority of the aliphatic carbon atoms (methylene groups), signal B to the methylene group next to the terminal methyl group, and signal C to the terminal methyl group of each aliphatic chain in the lipid molecule. The spectral line shapes are determined by scaled interaction tensors and reflect the characteristics of molecular motion.

spectra, are too weak to be identified. Signal A corresponds to the majority of the aliphatic carbon atoms (methylene groups), signal B to the methylene group next to the methyl group, and signal C to the methyl end group of each aliphatic chain in the lipid molecule. The spectrum is obtained at  $2.2^\circ$  deviation from the magic angle which causes all peaks to exhibit characteristic dynamic line broadening. However, all signals are well resolved and easy to assign to corresponding peaks of a high resolution spectrum (not shown). The lineshapes deviate significantly from simple Gaussian or Lorentzian functions; their overall widths strongly depend on the carbon position.

Corresponding spectral lineshape simulations were performed based on a numeric algorithm, which has been proposed

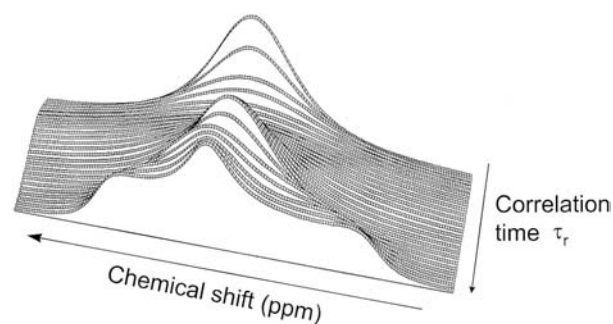


**Fig. 2.** A series of model calculations for the carbon spectrum of a terminal methyl group numerically derived under variation of the molecular tumbling rate  $\tau_r$ . With slow molecular tumbling rates (long correlation times  $\tau_r$  for isotropic rotational diffusion), the spectra in front ( $\tau_r = 15$  ms) reflect the features of a powder pattern for an asymmetric interaction tensor. With increasing rates, these characteristics get lost and an uncharacteristic wide line is obtained. With correlation times similar to the period of the sample rotation, the signal amplitudes go through a minimum and spectra become hardly detectable. Finally, at rapid tumbling, narrow lines are obtained independently of the velocity of sample rotation (last spectrum,  $\tau_r = 15$   $\mu\text{s}$ ).

for regular NMR spectra (9) and was adapted for sample spinning experiments (1). The sample spinning parameters (1660 Hz,  $52.5^\circ$ ) were determined by the experimental setup. The tensor elements for the local interaction, the anisotropies of the chemical shift, were not precisely known, therefore relevant data from a simple hydrocarbon molecule (n-icosane) were used instead (10). With these numbers given, the correlation time  $\tau_r$  for the isotropic rotational diffusion remains the only variable parameter. A typical result for a systematic variation of the correlation time (from 15 ms to 15  $\mu\text{s}$ ) for the chemical shift tensor of a methyl group is shown in Fig. 2.

The result summarized in Fig. 3 represents the best match between simulated and experimental spectra. Similar to the experimental spectrum, the contribution of spinning sidebands is insignificant. The fit was first optimized for the methyl signal C, then the resulting parameters were used to calculate the methylene peaks A and B. The relatively small deviations for signals A and B support the relevance of the data set, indicating a correlation time distribution between 0.1 ms and 1 ms. The

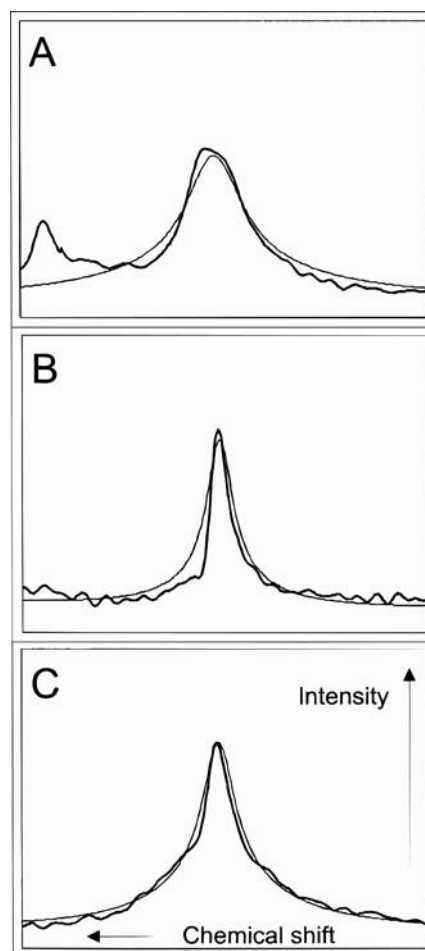


**Fig. 3.** Calculated best fits for three characteristic signals A, B and C of the experimental spectrum. The single parameter fit was first optimized for the terminal methyl group C, then the result was used to calculate peak A for the majority of the methylene groups and peak B for the methylene group next to the terminal methyl group of each aliphatic chain. The relatively small deviations for signals A and B support the relevance of the data set which indicates a correlation time distribution between 0.1 ms and 1 ms.

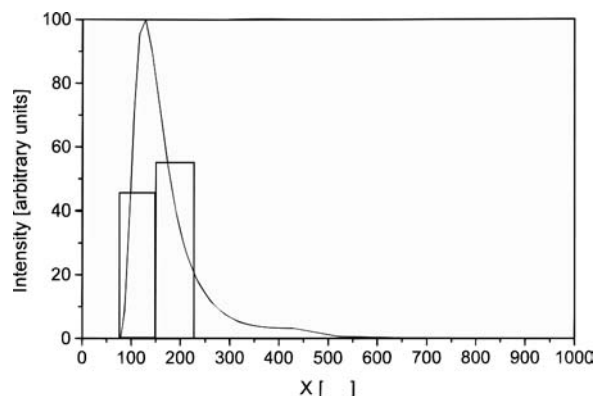


**Fig. 4** Particle size distributions of the SLN: —calculated from the photon correlation spectroscopy data by Contin program (8) □ (columns) calculated from rotational correlation times  $\tau_r$  as obtained by solid state NMR. The represented size distributions are number weighted.

size analysis by PCS represent the similarity of the particle distribution in the case of number and intensity weighted values. The distribution is relatively small (Fig. 4).

## DISCUSSION

With correlation times  $\tau_r$  between 0.1 ms and 1 ms for isotropic rotational diffusion, the SLN exhibit typical values for nanoparticles in aqueous suspension. Obviously, no inter- or intramolecular motion on this timescale is present within the particles. From a simple relation between the particle radius  $R$  and the rotational correlation time  $\tau_r$  given by (11)

$$\tau_r = \frac{4 \pi \eta R^3}{3 kT}$$

( $k$  being the Boltzmann constant) the particle radii can be estimated. With the viscosity of water given by  $\eta = 8.91 \cdot 10^{-4} \text{ Pa} \cdot \text{s}$  at  $T = 298 \text{ K}$  (12), the majority of particle diameters vary between 100 and 200 nm. Furthermore, it can be stated that the contributions of particles larger than 500 nm and smaller than 20 nm can be neglected, since neither a powder pattern in the sample spinning spectrum (Fig. 2, front) nor any motional narrowing in the static spectrum (not shown) are observed. These results are in good accordance with the corresponding data collected on a photon correlation spectrometer (Fig. 4), where the average (number weighted) of the particle diameter was determined as 170 nm with a polydispersity index of 0.15. Calculations based on the Contin procedure (8) indicate that the contribution of particles with diameters larger than 500 nm is well below 0.5%.

Different investigations show the influence of particle size for the organ distribution of intravenously injected particles (13–14). The SLN investigated in this case have a particle size distribution where the contribution of particles with diameters larger than 500 nm can be neglected. Therefore, these SLN will not be mechanically filtered by the capillary bed (about 6  $\mu\text{m}$ ) of the lung, will not lead to embolism and can be used for e.g. intravasal applications.

The mobility information obtained by solid state NMR also represents a valuable tool e.g. for the time resolved observation of release processes, since any dissolved component gives rise for a narrow signal which is easily separated from the original solid state spectrum. The time dependent signal intensities hereby allows to study the kinetics of the particle desintegration with respect to every single chemical constituent.

## CONCLUSIONS

This particle size analysis represents just an example of the versatility of the described method. The potential power of this method goes beyond this application; i.e. it allows for the determination of the chemical structure of liquid and solid components of almost any type of nanoparticles, e. g. polymer nanoparticles or liposomes while at the same time providing information about the mobility of individual chemical constituents. It is suitable for time resolved studies, e.g. for the observation of release processes or thermal degradation of particles. In combination with spin labeling, the sensitivity of this method is vastly increased, allowing studies on components present in low concentrations. These applications are presently under investigation and will be the subjects of future publications.

## ACKNOWLEDGMENTS

The authors thank Prof. Peter Pflögel for his general support and the valuable discussion on the content of this paper.

## REFERENCES

1. C. Mayer. Calculation of MAS spectra influenced by slow molecular tumbling. *J. Magn. Reson.* **139**:132–138 (1999).
2. A. C. Kolbert, P. J. Grandinetti, M. Baldwin, S. B. Prusiner, and A. Pines. Measurement of intermolecular distances by switched angle spinning. *J. Phys. Chem.* **98**:7936–7938 (1994).
3. S. Ding and C. A. McDowell. High resolution NMR spectra of nuclear spin systems under homogeneous interactions in solids exhibiting line narrowing induced by the memory effect. *J. Magn. Reson.* **117**:171–178 (1995).
4. S. Caldarelli, M. Hong, L. Emsley, and A. Pines. Measurement of carbon-proton dipolar couplings in liquid crystals by local dipolar field NMR in solids. *J. Phys. Chem.* **100**:18696–18701 (1996).
5. R. Challoner, R. K. Harris, and J. A. Tossell. Studies of an isolated  $^{15}\text{N}$ - $^{15}\text{N}$  spin pair. Off-angle fast-sample-spinning NMR and self-consistent-field calculations for diazo systems. *J. Magn. Reson.* **126**:1–8 (1997).
6. R. H. Müller, D. Rühl, S. Runge, K. Schulze-Forster and W. Mehnert. Cytotoxicity of solid lipid nanoparticles as function of lipid matrix and surfactant. *Pharm. Res.* **14**:458–462 (1997).
7. G. Lukowski and P. Pflögel. Electron diffraction of solid lipid nanoparticles loaded with aciclovir. *Pharmazie* **52**:642–643 (1997).
8. S. W. Provencher. Contin: A general purpose constrained regularization program for inverting noisy linear algebraic and integral equations. *Computer Physics Communications.* **27**:229–242 (1982).
9. C. Mayer. Lineshape calculations on spreadsheet software. *J. Magn. Reson.* **138**:1–11 (1999).
10. W. S. Veeman. Carbon-13 chemical shift anisotropy. *Prog. Nucl. Magn. Reson. Spectrosc.* **16**:193–235 (1984).
11. O. Södermann and U. Olsson. Micellar Solutions and Microemulsions. In D. M. Grant and R. K. Harris (eds.), *Encyclopedia NMR*, Wiley, 1995, pp. 3046–3057.
12. P. W. Atkins. *Physical Chemistry*, W. H. Freeman & Co, New York, 1994. C27 (Appendix).

13. M. Kanke, G. H. Simmons, D. L. Weiss, B. A. Bivins, and P. P. Deluca. Clearance of  $^{141}\text{Ce}$  labeled microspheres from blood and distribution in specific organs following intravenous and intraarterial administration in Beagle dogs. *J. Pharm. Sci.* **69**:755–762 (1980).
14. S. S. Davies, S. Douglas, L. Illum, P. D. E. Jones, E. Mak, and R. H. Müller. Targeting of colloidal carriers and the role of surface properties. In G. Gregoriadis, J. Senior and G. Poste (eds.), *Targeting of drugs with synthetic systems*. Plenum Press, New York, 1986, pp. 123–146.